BERKELEY LAB

Lawrence Berkeley National Laboratory

Data Analytics and Optimization of an Ice-Based Energy Storage System for Commercial Buildings

Na Luo, Tianzhen Hong, Hui Li, Ruoxi Jia,

Wenguo Weng

Energy Technologies Area
March, 2017

Acknowledgements

This work was supported by the Assistant Secretary for Energy Efficiency and Renewable Energy, [Building Technologies Program] or [Federal Energy Management Program], of the U.S. Department of Energy under Contract No. DE-AC02-05CH11231.

Data Analytics and Optimization of an Ice-Based Energy Storage System for Commercial Buildings

Na Luo[1,2], Tianzhen Hong[2,*], Hui Li[3], Ruoxi Jia[4], Wenguo Weng[1]

[1] Department of Engineering Physics, Tsinghua University, Beijing, China

[2] Building Technology and Urban Systems Division, Lawrence Berkeley National Laboratory, Berkeley, USA

[3] Shenzhen SECOM Technology Ltd., Shenzhen, China

[4] Department of Electrical Engineering and Computer Sciences, University of California, Berkeley, USA

*Corresponding author (T. Hong), thong@lbl.gov, 1(510)486-7082

Abstract

Ice-based thermal energy storage (TES) systems can shift peak cooling demand and reduce operational energy costs (with time-of-use rates) in commercial buildings. The accurate prediction of the cooling load, and the optimal control strategy for managing the charging and discharging of a TES system, are two critical elements to improving system performance and achieving energy cost savings. This study utilizes data-driven analytics and modeling to holistically understand the operation of an ice–based TES system in a shopping mall, calculating the system's performance using actual measured data from installed meters and sensors. Results show that there is significant savings potential when the current operating strategy is improved by appropriately scheduling the operation of each piece of equipment of the TES system, as well as by determining the amount of charging and discharging for each day. A novel optimal control strategy, determined by an optimization algorithm of Sequential Quadratic Programming, was developed to minimize the TES system's operating costs. Three heuristic strategies were also investigated for comparison with our proposed strategy, and the results demonstrate the superiority of our method to the heuristic strategies in terms of total energy cost savings. Specifically, the optimal strategy yields energy costs of up to 11.3% per day and 9.3% per month compared with current operational strategies. A one-day-ahead hourly load prediction was also developed using machine learning algorithms, which facilitates the adoption of the developed data analytics and optimization of the control strategy in a real TES system operation.

Keywords: thermal energy storage; optimization; data analytics; energy cost saving; heuristic strategy; machine learning

Acronym

TES	thermal energy storage
SQP	sequential quadratic programming
MPC	model-based predictive control
TOU	time of use
GA	genetic algorithm
COP	coefficient of performance
GPR	Gaussian processes regression
LR	linear regression
GRNN	generalized regression neural network
SVMR	support vector machine regression
RFR	random forest regression
RAE	relative absolute error
RRMSE	relative root mean square error
R^2	R-squared

1. Introduction

In recent decades, peak demand management of commercial buildings has become an active research area. Different strategies for shifting energy loads have been developed to reduce total operating costs without sacrificing the thermal comfort of building occupants. As noted in the report from the International Energy Agency, it is possible to gain an annual savings of $10—$15 billion for the U.S. market through peak demand management [1]. In general, load shifting control can be achieved using three strategies: building thermal mass, thermal energy storage (TES), and phase change materials. Recent reviews present and compare the current status of the three control strategies [2][3]; TES is the most widely used technology in existing air conditioning systems. A statistical study [4] shows that in the 1990s, about 1,500—2,000 units of TES cooling systems were employed in the U.S., of which the ice-based TES systems had the largest proportion of the market, at about 80%–85%. This sizeable market share for TES systems has increased interest in studying their operation.

In an ice-based TES system, cooling can be provided to meet the indoor thermal requirement either by directly operating the chiller or by discharging the ice storage. The chiller is also used to charge the ice storage during low-price electricity periods, which generally occur at night. The benefits of the TES system are twofold. First, a TES system can overcome the problem of constrained capacity that many current cooling systems face [5] from increasing occupant thermal comfort demand. With the help of an ice tank acting as a thermal battery, the whole system can not only meet a high-peak cooling demand during the hot season, but also possibly enhance its total performance and efficiency [6][7]. More importantly, by managing an appropriate allocation between the charging and discharging periods according to a time-of-use (TOU) electricity price, the total operating costs of chiller plant and TES system are significantly reduced [8][9].

Control strategies are often quite simple for most existing ice-based TES systems in buildings: these systems are either controlled manually, or are restricted to storage capacity-based control and priority-based control. Such conventional heuristic control strategies do not take full advantage of the available storage, and often lead to very limited cost savings [10]. Under these heuristic strategies, the ice storage solves the problem of high peak demand during the hot season; however, there is still huge potential to save more on operating costs by using an optimal control strategy. Indeed, the significant benefit of an optimal control strategy has been pointed out in previous studies that compared heuristic strategies [10][11]; specifically, these studies indicate that the benefits of the TES system could be maximized when the cooling loads are appropriately allocated in an optimal strategy.

Up until now, optimization studies for TES systems have mostly focused on physically modeling the thermal performance of the building and improving the efficiency of the cooling system by employing an optimal control or design strategy [12][13][14][15][16][17] [18][19]. For example, Cui et al. [12] developed a model-based optimal design method to optimize the capacity of the active cool storage while minimizing life-cycle costs for the system. Candanedo et al. [13]

described a model-based predictive control (MPC) approach for the cooling plant of a building. The MPC optimal strategy was compared with two rule-based strategies, resulting in a cost reduction of 5%-30%. Ma et al. [14] introduced an MPC approach to estimate the resulting electricity cost reductions in a university cooling system, using periodic invariant sets and dual-stage optimization to tackle feasibility issues with their proposed scheme. Lee et al. [15] presented an optimal design of an ice-based TES system, using particle swarm algorithms. This case study used minimal life cycle cost as the objective function to analyze the increase in power consumption and its potential influences on the system's optimization. Zhou et al. [16] developed an engineering approach to the optimal design of the water- and ice-based energy storage system in China, and evaluated the total annual cost. Lu et al. [17] developed an optimal scheduling strategy for a Zero Carbon Building in Hong Kong, using the MINLP method, reducing 25% of operational energy cost compared with a rule-based strategy. In these studies, different models and algorithms like Genetic Algorithm (GA) [9][11][20], Particle Swarm Optimization (PSO) [15][21], Mixed-integer Linear Programming (MILP) [18][22][23], and Mixed-integer Nonlinear Programming (MINLP) [17][24] were widely used to solve the optimization problem. Two previous reviews introduced these optimization techniques in the context of TES operations [25][26]. Given new trends of data collection and data analytics, however, an optimal control strategy can now be developed using a real performance dataset, by first evaluating the system's current operating status and subsequently improving the performance to achieve the system's full savings potential. This data-driven solution can more accurately solve the optimization problem for the given TES system.

This study presents a new approach and workflow for pairing data-driven analytics with modeling to understand the operation of an ice-based TES system in a shopping mall, and to calculate the performance of the equipment in the central cooling plant. Based on this calculated performance, the study develops a novel optimal control strategy that achieves minimum operating costs for cooling; the energy costs savings potential of the strategy is finally compared with three conventional heuristic strategies, assuming three scenarios of cooling demand level. The datasets used in this work were from actual measurements from installed meters and sensors in the TES system. As the optimization of TES requires the cooling load profile to be known *a priori*, we also propose a cooling load prediction algorithm based on Gaussian process regression, which can provide an accurate forecast of the cooling load using weather data. Overall, the study demonstrates a holistic approach to optimizing the operation of a TES system in a real air-conditioning system.

2. Description of the TES system and the dataset

The ice-based TES system of focus provides partial cooling for a shopping mall in Shenzhen, a city located in Southern China. The shopping mall has four stories with a total conditioned floor area of 35,000 m^2. The dataset includes measured parameters for the central cooling plant equipment and the cooling energy demand of the shopping mall. The source data were recorded at irregular time intervals and were thus consolidated into hourly data. The data were

recorded from June to November 2016, covering the cooling season from late spring to early winter in Shenzhen.

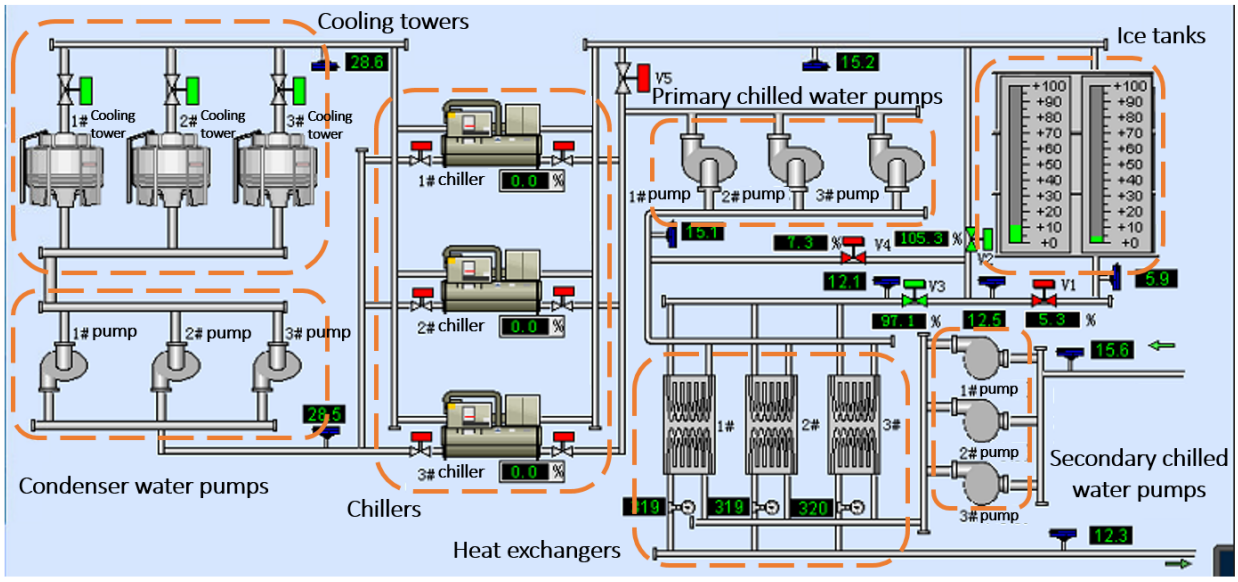

Figure 1 System diagram of the central cooling plant

Figure 1 shows the system diagram of the central cooling plant. Table 1 shows the performance parameters for each piece of equipment in this TES system.

There are three identical York chillers (YSQXEXS45CJE) with screw compressors using R-22 refrigerant. The chillers are dual-operational, either providing the cooling or making ice to charge the ice tank. Due to the electric current limit of the whole system, only two chillers are designed to operate simultaneously. The third chiller is used for backup during extremely hot conditions. For each chiller, during the direct cooling stage, the capacity is rated at 1,337 kW with a power input of 252 kW (COP = 1,337/252 = 5.31). During the ice-charging stage, the capacity is rated at 823 kW with a power input of 213 kW (COP = 823/213 = 3.86).

The cooling system also consists of three identical cylindrical tanks to store the ice. The total storage capacity is 5,500 RT (19,343.5 kW), which is lower than the daily cooling demand most of the time. The ice tanks are installed in the basement with good insulation, which significantly reduces the heat gains to the tanks; accordingly, we ignored these heat gains in this study. The ethylene glycol refrigerant for making the ice is transported through three circulation pumps. There are four types of operating modes in this system, which are: direct cooling by the chillers, direct cooling by the ice tank, combined cooling by the chillers and the ice tank, and charging the ice tank by the chillers. Four valves with different combinations of opening and closing are used to switch between these four different operating modes.

In addition, there are three groups of cooling towers with three condenser water pumps for delivering the condenser water. Three primary and secondary chilled water pumps are used to

deliver chilled water to the building. Several temperature sensors were installed in this system to measure the inlet and outlet water temperature for each part of the cooling system. The total flow rate of the chilled water was also measured.

Table 1 Performance parameters for each piece of equipment in the central plant

Brand & Model	Number of units	Type	Refrigerant type	Refrigeration capacity（kW）	Power input (kW）	Chilled water flow rate（m^3/h)	Condenser water flow rate（m^3/h)
York YSQXEXS 45CJE	3	Screw compressors	R22	1,337 (high)	252	248	273
				823 (low)	213	248	273

Brand & Model	Model	Number of units	Capacity (m^3/h)	Head (m)	Electric power (kW)
WEI NU, Secondary chilled water pumps	NL125/315-30/4	3	275	28	30
Primary chilled water pumps	NL150/400-45/4	3	275	38	45
WEI NU, Condenser water pumps	NL125/315-37/4	3	290	28	37

Brand	Number of units	Transverse flow/Counter flow	Circulation water flow rate (m^3/h)	Electric power (kW)
SINRO cooling towers	3	Transverse flow	300	7.5

Brand	Number of units	Length (m)	Width (m)	Height (m)	Capacity (RT)
Ice storage tank	3	7.8	4.6	3.768	5,500 (19,343.5 kW)

3. Methodology

Figure 2 shows the study's overall methodology. First, the datasets were analyzed to help understand the current control strategy and the operational performance of each piece of equipment. Resultant performance curves can be used to accurately calculate the total energy costs of the TES system under various control strategies. Three heuristic strategies, including

chiller-priority, ice-priority, and price-priority, were used to calculate operating energy costs; the limitations and saving potentials of each strategy were also evaluated. In parallel, an optimal strategy was developed to better allocate flexible cooling loads to the chillers and ice tanks, with an objective of minimizing total operating costs. To solve the optimization problem, an objective function and constraint conditions were determined based on the performance analysis described above. Subsequently, an appropriate algorithm was selected for the optimization problem and implemented. Finally, the results from all five control strategies were compared and analyzed further.

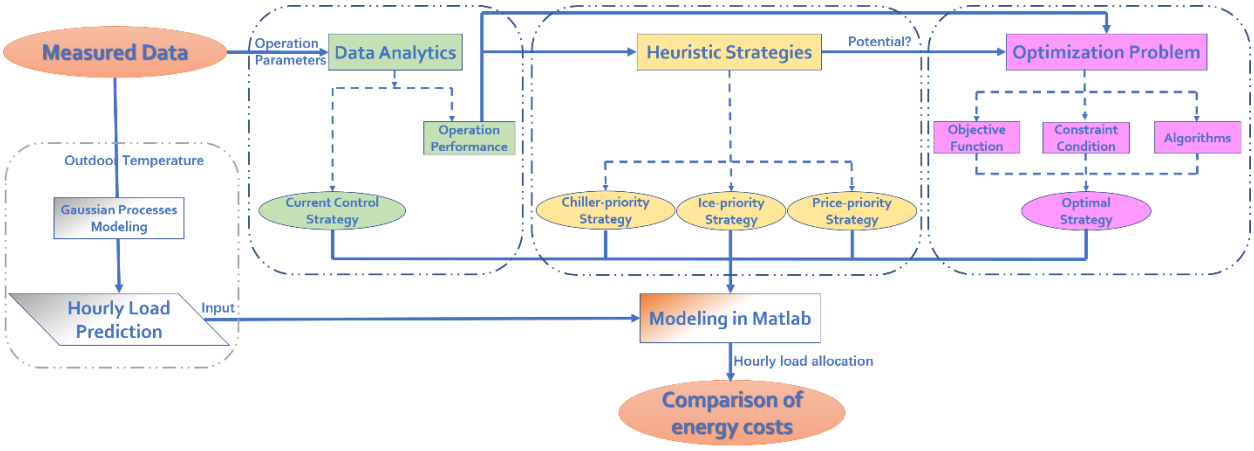

Figure 2 The overall methodology of the data analytics, modeling, and optimization

3.1. Data analytics

3.1.1. Electricity rates

Figure 3 shows the TOU electricity rate profile in Shenzhen city. The rate profile peaks at 1.1147 RMB/kWh during the periods of 9:00–12:00, 14:00–16:00, and 19:00–21:00. The lowest electricity rates are 0.2788 RMB/kWh during the night period of 23:00–8:00. For the other time periods, the electricity rate is 0.8959 RMB/kWh. It can be seen that the rate during the nighttime is much lower than that during the daytime; this pricing characteristic favors the use of load shifting management to reduce operating costs.

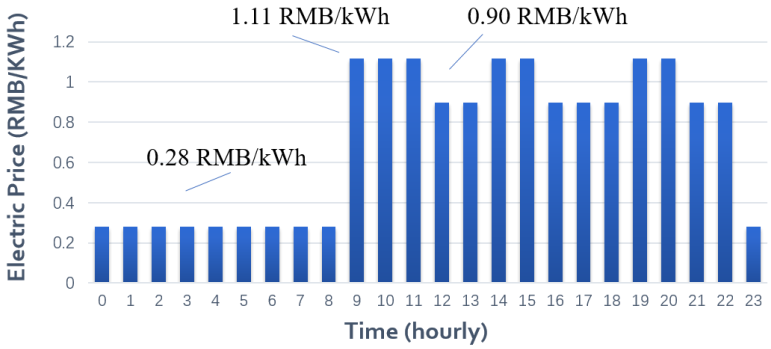

Figure 3 Daily 24-hour electricity rate profile in Shenzhen city

3.1.2. Data pre-processing

Time correspondences for different parameters are very important in this work. First, to understand the current hourly control strategy, the open status of each valve must be compared at the same hour, to discover their different combinations. Second, to calculate the hourly cooling load, temperature differences and water flow rate must be used at the same hour as well. However, the measured data are somewhat irregular in time – specifically, the time was unevenly divided into 35 time periods per day, leading to difficulties in building the correlations between different parameters across time. Ultimately, irregular interval data were consolidated into hourly data by mapping the time point to the adjacent hour; overlapping values within the same hour were averaged out.

3.1.3. Current operation strategy

Table 2 shows the four major valves, their combinations, and corresponding operation modes. Furthermore, Figure 4 (a) shows the four major valves controlling the different operation modes on the system diagram. The open status of both V2 and V3 represents the operating mode of direct cooling by the chillers, the open status of both V1 and V3 represents a direct cooling operating mode by the ice tanks, while the open status of both V1 and V4 represents charging of the ice tank by the chillers. Occasionally, when the cooling demand is very high during the hot seasons, the chillers and the ice tanks were used together under the combined open status of V1, V2, and V3.

Table 2 Different operation modes and combinations of valves status (√ : opened, ×: closed)

Operation modes	V1	V2	V3	V4
Charge the ice tank	√	×	×	√
Direct cooling by chillers	×	√	√	×
Direct cooling by ice tank	√	×	√	×
Combined cooling by chillers and ice tank	√	√	√	×

In this work, Tableau version 10.1.1 was applied to further analyze and visualize the current operation strategy. Tableau is specialized software for analyzing relational databases, and is widely used in the data analytics research area. Figure 4(b) shows the system's current operating strategy for one typical day (July 1, 2016). Here, different color bars represent different operational modes during the hour. The electric rate profile and the total cooling load are also presented in Figure 4(b), for reference. Compared against the electric rate profile shown below, the current strategy can be considered a "price-priority" strategy. The ice tank

was charged during the night based on a load prediction, when the price was low; during working hours in the daytime, when the price was on-peak, the ice tank was discharged to provide cooling; otherwise, the chillers were operating. When the cooling demand was relatively high at time 17:00, the chillers and the ice tank were operating together.

The current control strategy was not completely in line with the variation of the electricity price all the time, however, due to the use of manual control. Indeed, to satisfy cooling demand and avoid sacrificing the occupants' thermal comfort, chillers were preferred to the ice tank, even during the on-peak electricity rate periods. In this case, the ice stored during the night was not fully discharged during the daytime, increasing total energy costs.

(a)

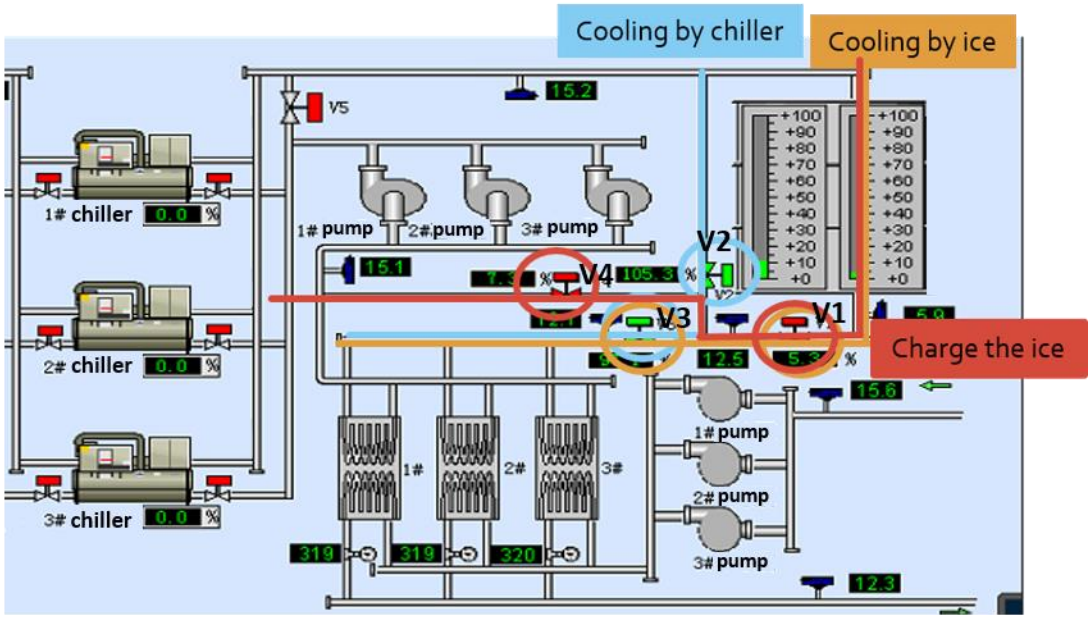

(b)

Figure 4 (a) System diagram with operation modes, (b) Current operating strategy (one typical day, July 1, 2016)

3.1.4. Equipment performance curves

The total cooling load can be calculated based on the equation below:

$$Q_{total} = c\rho V(T_{inlet} - T_{outlet}) \quad \text{Eq. 1}$$

where Q_{total} is the total cooling load of the entire system; c and ρ are the specific heat capacity and density of the water, respectively; V is the hourly measured flow rate of the chilled water; and $T_{inlet} - T_{outlet}$ represents the measured temperature difference of the chilled water in one hour.

Using the different combinations of the valve open status shown in Figure 4, operating periods for the chillers and ice tanks were separately identified. Thus, the actual cooling load provided by chiller-only and ice-only could be calculated. Divided by the corresponding measured electricity use for each hour, the efficiency for each piece of equipment was calculated during daytime operating hours, based on the following equations:

$$COP_{chiller} = \frac{cooling\ load_{chiller}}{energy\ consumption_{chiller}} \quad \text{Eq. 2}$$

$$COP_{ice} = \frac{cooling\ load_{ice}}{energy\ consumption_{ice}} \quad \text{Eq. 3}$$

$$COP_{pump} = \frac{cooling\ load_{pump}}{energy\ consumption_{pump}} \quad \text{Eq. 4}$$

$$COP_{cooling\ tower} = \frac{cooling\ load_{cooling\ tower}}{energy\ consumption_{cooling\ tower}} \quad \text{Eq. 5}$$

where $COP_{chiller}$ and COP_{ice} (coefficient of performance) represent the ratio of electricity supplied to satisfied cooling load for the chillers and the ice tanks, respectively; COP_{pump} and $COP_{cooling\ tower}$ represent the water-to-wire efficiency of pumps and cooling towers related to the cooling load satisfied by the chillers.

Equipment performance curves can be determined based on the equipment's calculated COP and cooling load to establish correlations between cooling efficiency and cooling load. 0 shows the performance curves for (a) the chillers, (b) the ice tanks, (c) the pumps, and (d) the cooling towers. The x-axis in 0 (a) is the load ratio, or the cooling load divided by the capacity of a single chiller. The chiller performance curve is a power function with an R-squared value of 0.9066. For the ice tank in 0 (b), the COP was almost irrelevant to the ice content or cooling load; thus, the constant average COP of 40 for the ice tanks was determined. Finally, although the cooling towers have variable speed fans, they operate at constant power due to the installation of an enclosure to reduce the operating noise. Therefore, as shown in 0 (d), the electricity consumption of the cooling towers remained constant during operation.

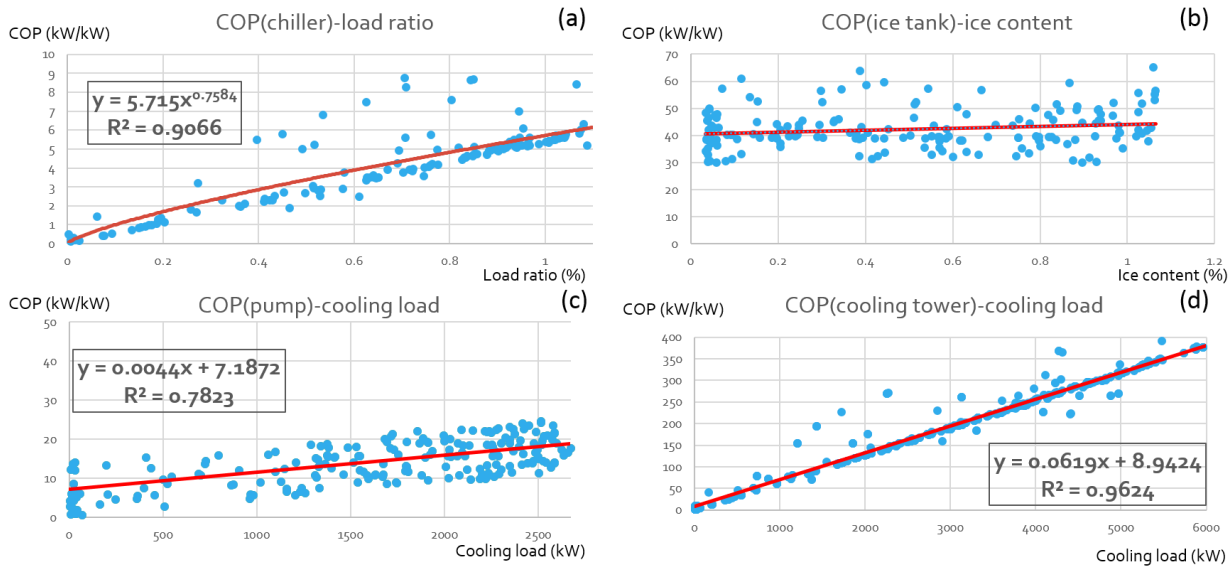

Figure 5 Performance curves for (a) chillers, (b) ice-tanks, (c) pumps, and (d) cooling towers

3.2. Heuristic strategies

TES operating strategies are generally classified as either full storage or partial storage, referring to whether the storage capacity is large enough to support the total amount of cooling demand during on-peak hours. The cooling capacity of the current ice tank is much lower than the designed cooling demand, which makes it a partial storage system. Nowadays, for most partial storage systems, three heuristic strategies are widely used to control the operation, including the chiller-priority strategy, the ice-priority strategy, and the price-priority strategy.

3.2.1. Chiller-priority strategy

For the chiller-priority strategy, chillers are designed to operate all the time. During the on-peak periods when the cooling demand exceeds the chiller capacity, the ice tank will be discharged to meet the remaining cooling load. During the night, three chillers will be operated at full capacity to charge the ice tank until they reach the needed ice amount for daytime use. Figure 6 (a) shows the schematic diagram of the chiller-priority strategy.

3.2.2. Ice-priority strategy

For the ice-priority strategy, the ice tank is utilized to meet the cooling load during the first few operating hours. Here, the chillers start to operate after the ice runs out. When the cooling demand exceeds the cooling capacity of the two chillers, the third chiller is then put into use to meet the remaining load. During the night, the three chillers will be operated at full capacity to charge the ice tank until they reach the daily needed ice amount. The schematic diagram of the ice-priority strategy is shown in Figure 6 (b).

3.2.3. Price-priority strategy

The operating modes of the price-priority strategy depend on the hourly electricity price, as shown in Figure 3. The ice tank is first discharged when the electricity price is high. Otherwise, when the electricity price is relatively low, the chillers are used to meet the cooling load. Similar to the ice-priority strategy, when using the two chillers and ice storage does not satisfy the cooling demand, a third chiller will be used to meet the remaining cooling load. Figure 6 (c) shows the schematic diagram of the price-priority strategy.

Figure 6 Diagram of three heuristic strategies: (a) chiller priority, (b) ice priority, and (c) price priority

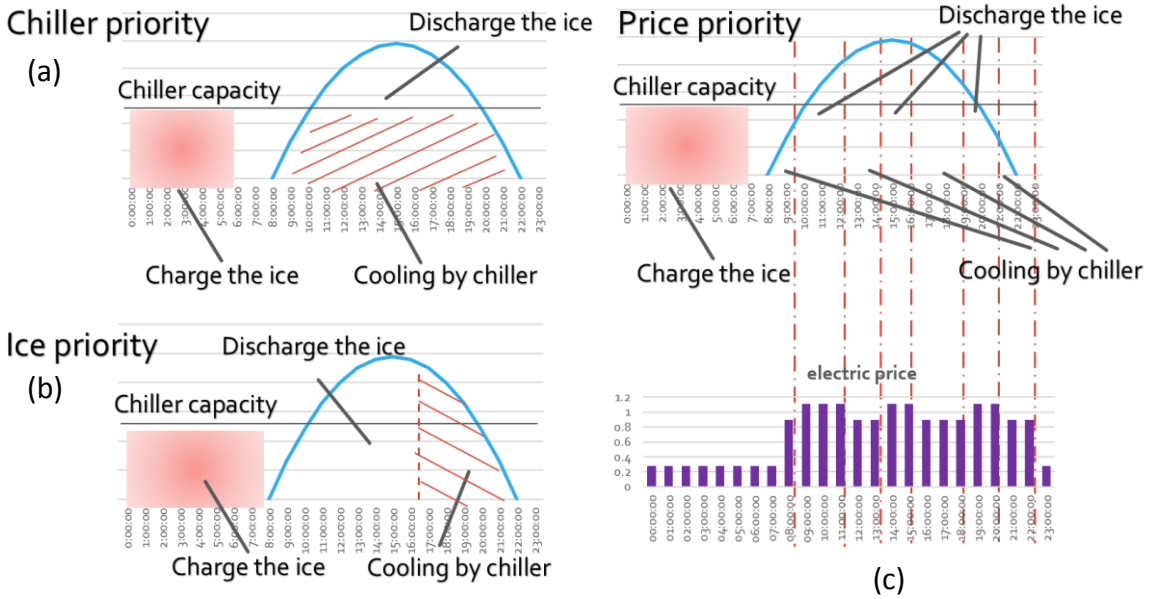

3.3. Optimal strategy

On top of the conventionally used heuristic strategies described above, an optimal TES operating strategy can be developed and evaluated by forming and soling an optimization problem using the derived equipment performance curves, the actual electricity TOU rates, and the hourly cooling demand.

3.3.1. Objective function

The objective of the current optimization problem is to minimize the operating costs of the cooling system by appropriately allocating the cooling load for the chillers and the ice tank. In an optimal control scenario, the objective function must apply to each unique operational period. Accordingly, in this work, the objective function was defined ($M = min \sum_{i=0}^{23}(e_i \times E_i) = min\left\{\sum_{i=9}^{22}(e_i \times \left(\frac{X_i}{COP_{chiller}} + \frac{X_i}{COP_{pump}} + \frac{X_i}{COP_{cooling\ tower}}\right)) + \sum_{i=9}^{22}\left(e_i \times \frac{Y_i}{COP_{ice}}\right) + \sum_{i=23}^{8}(e_i \times f_i(\sum Y_i))\right\}$ Eq. 6) by separately considering the chiller operating periods during the daytime and the ice tank charging and discharging during night and daytime, respectively.

$$M = min\sum_{i=0}^{23}(e_i \times E_i) = min\left\{\sum_{i=9}^{22}(e_i \times \left(\frac{X_i}{COP_{chiller}} + \frac{X_i}{COP_{pump}} + \frac{X_i}{COP_{cooling\ tower}}\right)) + \sum_{i=9}^{22}\left(e_i \times \frac{Y_i}{COP_{ice}}\right) + \sum_{i=23}^{8}(e_i \times f_i(\sum Y_i))\right\} \quad \text{Eq. 6}$$

where *M* represents the targeting minimal total daily operating cost of the entire TES system (RMB); *e* and *E* are the electric price (RMB/kWh) and electricity consumption (kWh), respectively; and *i* represents the *i*th hour of a day. The business hours of the shopping mall are from 9:00 am to 10:00 pm and the charging periods start afterward. *X* and *Y* represent the cooling load (kW) met by the chillers and the ice tank, respectively. $COP_{chiller}$, COP_{pump}, and $COP_{cooling\ tower}$ have been described by the cooling load of chiller (X_i) and the ice tank (Y_i), (0 (a–d)); this optimization finds a non-linear optimization solution.

3.3.2. Constraint conditions

It is noted that there are certain constraints on X_i and Y_i. In particular, during the daytime, the total cooling loads provided by the chillers and the ice tank must satisfy the total cooling demand during that period of time. Moreover, the cooling load provided by one chiller must not exceed or be less than 20% of its rated capacity, considering the chiller's minimum limit of operating hours. Since there are two chillers operating at the same time, the capacities of the two chillers were considered separately. Finally, the ice tank's discharging rate must not exceed a maximum melting amount within one hour. Such constraints are represented in $\sum(X_{i,1} + X_{i,2} + Y_i) = Q_{i,total}$ Eq. 7–$0 \le Y_i \le Y_{imax}$ Eq. 10 as follows.

$$\sum(X_{i,1} + X_{i,2} + Y_i) = Q_{i,total} \quad \text{Eq. 7}$$

$$267 \le X_{i,1} \le 1337 \quad \text{Eq. 8}$$

$$267 \le X_{i,2} \le 1337 \quad \text{Eq. 9}$$

$$0 \le Y_i \le Y_{imax} \quad \text{Eq. 10}$$

where Y_{imax} represents the maximum melting amount (kW) at the *i*th hour, which depends on the total discharging cooling load during previous hours. The previous total cooling capacity (Q, kWh) was described as an exponential function of time (h), as shown in $Q = 19343.5 \times (1 - e^{-0.316t})$ Eq. 11, which was based on the performance parameter of the ice-storage system.

$$Q = 19343.5 \times (1 - e^{-0.316t}) \quad \text{Eq. 11}$$

where 19343.5 is the total capacity of the ice tank, and 0.316 is an empirical parameter of the tank.

Y_{imax} can be determined as:

$$Y_{imax} = \frac{dQ}{dt} = 6112.55 \times (1 - \frac{\sum_{k=1}^{i-1} Y_k}{19343.5}) \quad \text{Eq. 12}$$

Measured data were used to verify the accuracy of $Q = 19343.5 \times (1 - e^{-0.316t})$ Eq. 11. When the cooling demand is provided only by the ice tank, Figure 7 shows that the cooling load (y-axis) and its corresponding ice content percentage (x-axis) can be analyzed. Assuming that the ice content percentage varies linearly with the tank capacity, according to the empirical formula, the theoretical maximum cooling load can be described as $load_{max} = 6112.55 \times (1 - \mathrm{x}\%)$, which is shown as the orange line in Figure 7. It can be seen from the figure that, for each level of the ice content percentage, all the actual operating cooling loads are beneath (or equal to) the theoretical maximum cooling load. Therefore, the measured performance data proved that $Q = 19343.5 \times (1 - e^{-0.316t})$ Eq. 11 is valid in representing the maximum cooling rate constraint condition for the ice tank.

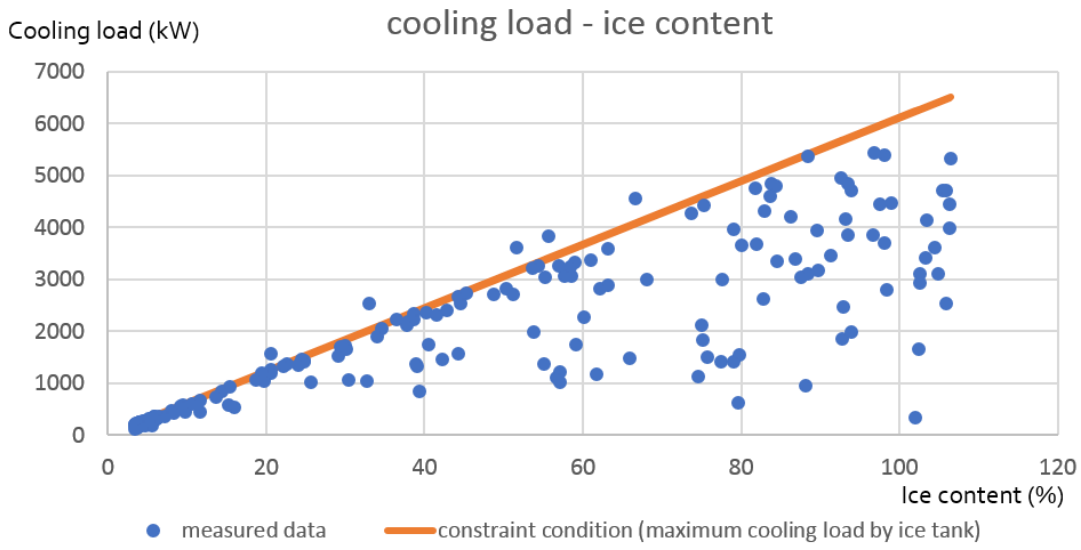

Figure 7 Comparison between actual cooling load and constraint condition for the ice tank

During the night, when the chillers were operated to charge the ice tank, Figure 8 shows that electricity consumption was related to stored ice content. Thus, the f_i in the objective function can be described as in $f_i = 6466 \times \frac{\sum Y_i}{19343.5} + 903.6$ Eq. 13:

$$f_i = 6466 \times \frac{\sum Y_i}{19343.5} + 903.6 \qquad \text{Eq. 13}$$

where f_i is the electricity consumption for charging (kWh) the ice tank, and $\sum Y_i$ represents the total cooling load provided by the ice tank during the daytime.

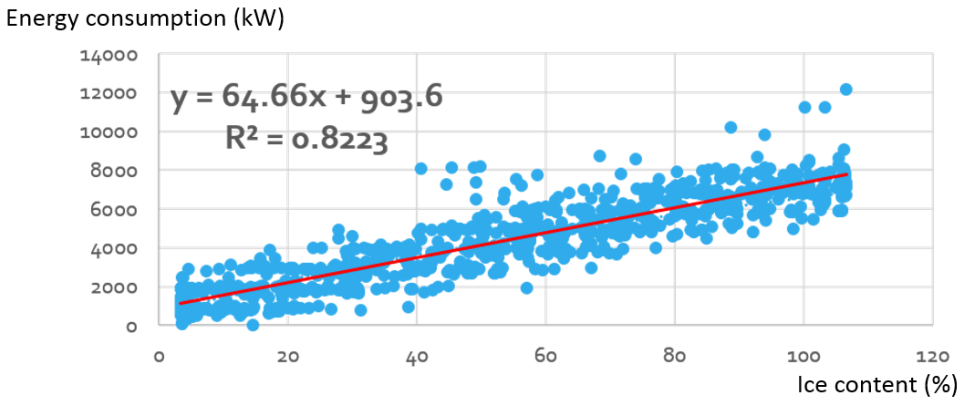

Figure 8 Fitted curve for measured ice tank electricity consumption and ice content during the night

3.3.3. Optimization algorithms

To solve the nonlinear objective function, a Sequential Quadratic Programming (SQP) method was used. SQP is an iterative method for solving a nonlinear optimization, especially for which the objective function and the constraints are twice continuously differentiable. This method solves a sequence of optimization sub-problems, each of which optimizes a quadratic model of the objective subject to a linearization of the constraints [27]. Global search was also used to find a global optimal solution to this problem.

The initial value of the SQP algorithm was determined as the output of the price-priority strategy to save on computation time. A genetic algorithm (GA) was also tested as an effective way to obtain the initial values. The calculated results for both methods were found to be insensitive to initial values and only related to the boundary constraint conditions.

In this work, Matlab release 2015 was applied on a normal PC with Windows 7 to perform the modeling of the three heuristic strategies and the optimal strategy.

3.4. Load prediction model

We present a cooling load prediction method based on Gaussian processes regression (GPR), a powerful non-parametric machine learning algorithm. The Gaussian process has been successfully applied to tasks such as prediction of electricity demand [28], atmospheric carbon dioxide concentration [29], and robotics dynamics [30]. In this study, we will show the flexibility and ability of GPR to provide an accurate prediction with a relatively small dataset.

3.4.1. Background overview of GPR

Let $D = \{(x_1, y_1), \cdots, (x_n, y_n)\}$ be a set of n training samples drawn from a noisy process:

$$y_i = f(x_i) + \epsilon \qquad \text{Eq. 14}$$

where each x_i is an input sample and y_i is a target value. The noise ϵ is assumed to come from a zero mean Gaussian distribution with some variance σ_n^2. A key idea underlying GPR is the

requirement that the target values at different points are correlated, where the covariance between two function values, $f(x_i)$ and $f(x_j)$, hinges on the corresponding input values x_i and x_j through an arbitrary covariance function, or kernel $k(x_i, x_j)$, i.e., $cov\left(f(x_i), f(x_j)\right) = k(x_i, x_j)$. The GPR assumes that the target values evaluated at any collection of input samples are drawn from a joint Gaussian distribution with mean and covariance functions evaluated at the inputs. For notation convenience, we denote $(x_1, \cdots, x_n)$ by $\boldsymbol{x}$, and $(y_1, \cdots, y_n)$ by $\boldsymbol{y}$; then GPR indicates $\boldsymbol{y} \sim N(m(\boldsymbol{x}), K(\boldsymbol{x}, \boldsymbol{x}) + \sigma_n^2 \boldsymbol{I})$ where $[K(\boldsymbol{x}, \boldsymbol{x})]_{i,j} = k(x_i, x_j)$. We are interested in predicting the function value at an arbitrary point x^*, conditioned on the training data $\boldsymbol{x}$ and $\boldsymbol{y}$. From the GPR assumption, the posterior over the function values f^* at x^* is Gaussian, distributed according to $N\left(\overline{f^*}, cov(f^*)\right)$, where:

$$\overline{f^*} = E[f^* | \boldsymbol{x}, \boldsymbol{y}, x^*] = K(x^*, \boldsymbol{x})[K(\boldsymbol{x}, \boldsymbol{x}) + \sigma_n^2 \boldsymbol{I}]^{-1} \boldsymbol{f} \qquad \text{Eq. 15}$$

$$cov(f^*) = K(x^*, x^*) - K(x^*, \boldsymbol{x})[K(\boldsymbol{x}, \boldsymbol{x}) + \sigma_n^2 \boldsymbol{I}]^{-1} K(\boldsymbol{x}, x^*) \qquad \text{Eq. 16}$$

Therefore, $\overline{f^*}$ can be used as the prediction at x^*.

Similar to other machine learning algorithms, the use of GPR in any prediction tasks is accomplished in two phases: namely, training and testing. In the training phase, a dataset consisting of input samples and corresponding target values is utilized to select the hyper-parameters of the kernel function. Once the kernel function is learned, it can be used for predicting the target values for new input samples in the testing phase.

3.4.2. GPR for cooling load prediction

The dataset available for cooling load prediction consists of hourly time-stamped outdoor air wet-bulb temperature and the hourly cooling load derived from in situ measurements of supply and return water temperature and water flowrate. Our goal is to model the cooling load as a function of time and weather parameters. The cooling load data during a randomly chosen time interval is shown in Figure 9 (a), where we can observe a pronounced daily and weekly periodicity of the cooling load. Figure 9 (b) demonstrates the impact of the wet-bulb temperature on the cooling load. The linear line fit to the temperature and cooling load data shows that the increase in temperature generally tends to increase the cooling load. The observations from the Figure 9 (a) and Figure 9 (b) inspire our design of the kernel function as follows.

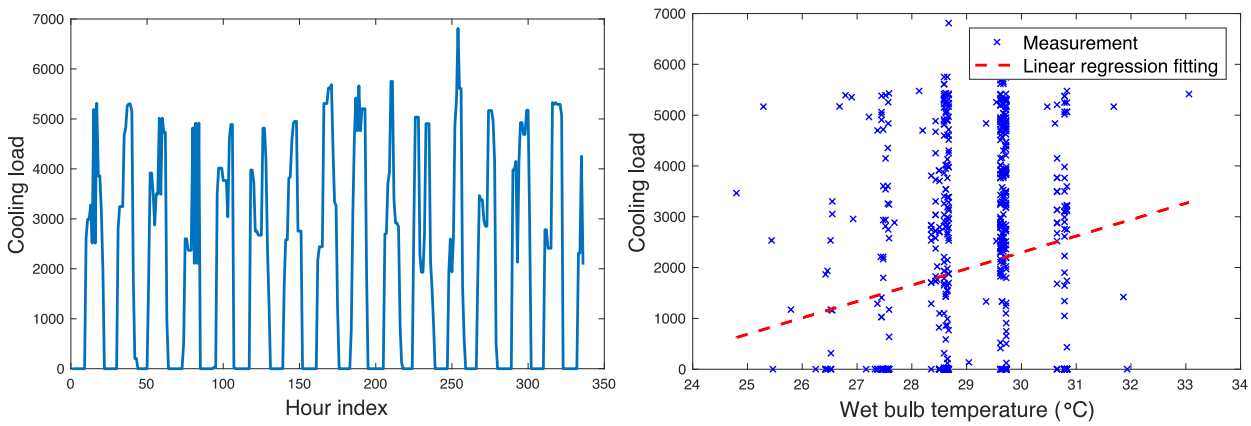

(a) (b)

Figure 9 The impact of (a) time and (b) temperature on the cooling load: (a) the cooling load data during a randomly chosen 2-week long time window in the training dataset, and (b) the correlation between temperature and cooling load with a linear line fitting.

To incorporate the "hourly effect" that allows each hour of the day to have a different predicted load, and the "day effect" that allows each day of the week to have a distinctive predicted load, we map the data time stamps to an hourly index within a day, and the day index to a week. The ith input sample is given by:

$$x_i = [HI_i, DI_i, T_i] \qquad \text{Eq. 17}$$

where HI_i and DI_i stand for the hour and day index, respectively. T_i indicates the outdoor air wet-bulb temperature measurement.

To model the "hourly effect", we use the periodic covariance form, multiplied with a squared exponential component to allow a possible decay from exact periodicity:

$$k_1(HI_i, HI_i') = \theta_1 \exp\left(-\frac{(HI_i - HI_i')^2}{2\theta_2^2} - \frac{2\,sin^2\left(\frac{\pi(HI_i - HI_i')}{p_1}\right)}{\theta_3^2} \right) \qquad \text{Eq. 18}$$

where p_1 is the period of the covariance function, which is initialized to be 24. θ_1 gives the magnitude, θ_2 is the decay time for the periodic component, and θ_3 defines the smoothness of the periodic component.

Similarly, we model the "day effect" by a decayed periodic covariance function given by:

$$k_2(DI_i, DI_i') = \theta_4 \exp\left(-\frac{(DI_i - DI_i')^2}{2\theta_5^2} - \frac{2\,sin^2\left(\frac{\pi(DI_i - DI_i')}{p_2}\right)}{\theta_6^2} \right) \qquad \text{Eq. 19}$$

where p_2 is initialized to be 7.

The impact of wet-bulb temperature on the cooling load is capture by the sum of a squared exponential term and a rational quadratic term:

$$k_3(T_i, T_i') = \theta_7^2 \exp\left(-\frac{(T_i - T_i')^2}{2\theta_8^2}\right) + \theta_9^2 \left(1 + \frac{(T_i - T_i')^2}{2\theta_{10}\theta_{11}^2}\right)^{-\theta_{10}} \quad \text{Eq. 20}$$

where the squared exponential term is used to capture the smoothly increasing trend, and the rational quadratic covariance term is to model irregularities.

To capture the impact of the "hourly effect," "daily effect," and temperature on cooling load, the final kernel function used in the GPR-based load prediction is the sum of the aforementioned kernel functions:

$$k(x_i, x_i') = k_1(HI_i, HI_i') + k_2(DI_i, DI_i') + k_3(T_i, T_i') \quad \text{Eq. 21}$$

The parameters of the covariance function are learned from the training dataset by maximizing the log-likelihood of the training dataset. Interested readers are referred to [29] for more details on the derivation of the training procedure.

4. Results

4.1. Daily analysis for three typical cooling demand scenarios

The optimal and three heuristic strategies were investigated under three typical scenarios with different levels of daily total cooling loads. Due to the different cooling demand levels, the performance and savings potential of the optimal strategy tends to be different than for the three heuristic strategies. Examining the underlying datasets, the lowest cooling demand for the current system was more than 20,000 kWh per day; average-level cooling demand was nearly 40,000 kWh per day; and high-level cooling demand was almost 50,000 kWh. In this context, three "typical" days were selected to represent three scenarios of cooling demand level; these were the minimum level on October 10, the average level on July 2, and the maximum level on August 5. The total operating energy costs for the three scenarios were calculated and are listed in Table 3. It should be noted that only as many as two chillers were allowed to operate simultaneously.

Table 3 Total energy costs (RMB) of different control strategies under three scenarios (maximally two chillers operating)

	Minimum load (A)	**Average load (B)**	**Maximum load (C)**
Date	October 10	July 2	August 5
Current	5951.00	7563.66	8228.46
Optimal	5309.47	7113.01	7757.34
Chiller priority	7923.82	8922.32	9268.26
Ice priority	5758.55	**6951.33***	**7152.71***
Price priority	5831.59	**7364.04***	**7781.85***

[*] These simulated results are yielded under the assumption that only up to two chillers can operate simultaneously; this assumption led to some hours with loads not met, potentially failing to satisfy occupant comfort. Separate simulations were run assuming all three chillers can operate simultaneously, and updated results are listed in Table 4.

4.1.1. Minimum level of cooling loads

Figure 10 shows the calculated allocation of the cooling load, to both the chillers and the ice tank, for different control strategies under the minimum-level load scenario. From the daily energy cost in column A of Table 3, it can be seen that the optimal strategy reduces energy costs up to 10.8% compared to the current control strategy, which is similar to a price-priority scheme. Of all the five strategies, the cooling loads were assumed to be 100% met by the chillers or ice tanks, and the chiller-priority strategy cost the most. The capacity of the ice-storage system was much less utilized with the chiller-priority strategy, especially under the minimum-load scenario, when two chillers can meet the majority of the cooling demand. The price-priority strategy can avoid using the chillers during the on-peak price periods in principle; however, depending on the level of the cooling demand, the utilization rate of the ice storage was still limited under this scenario. As for the optimal and ice-priority strategies, they both save more energy costs by taking full advantage of the ice-storage capacity. The ice tank was fully charged during the night, when the electric price was much lower; during the daytime operating hours, the ice tank could provide much more cooling with a higher efficiency (only pumps consumed electricity) than that provided by the chillers. Therefore, the total operating costs can be reduced if the ice tank is fully used during the high electricity price periods. As shown in Figure 10, between the optimal and ice-priority strategies at time 20:00, the optimal strategy performed better than the ice-priority strategy in accurately avoiding running the chillers during the on-peak price periods, which made it the most economical strategy among all five control strategies.

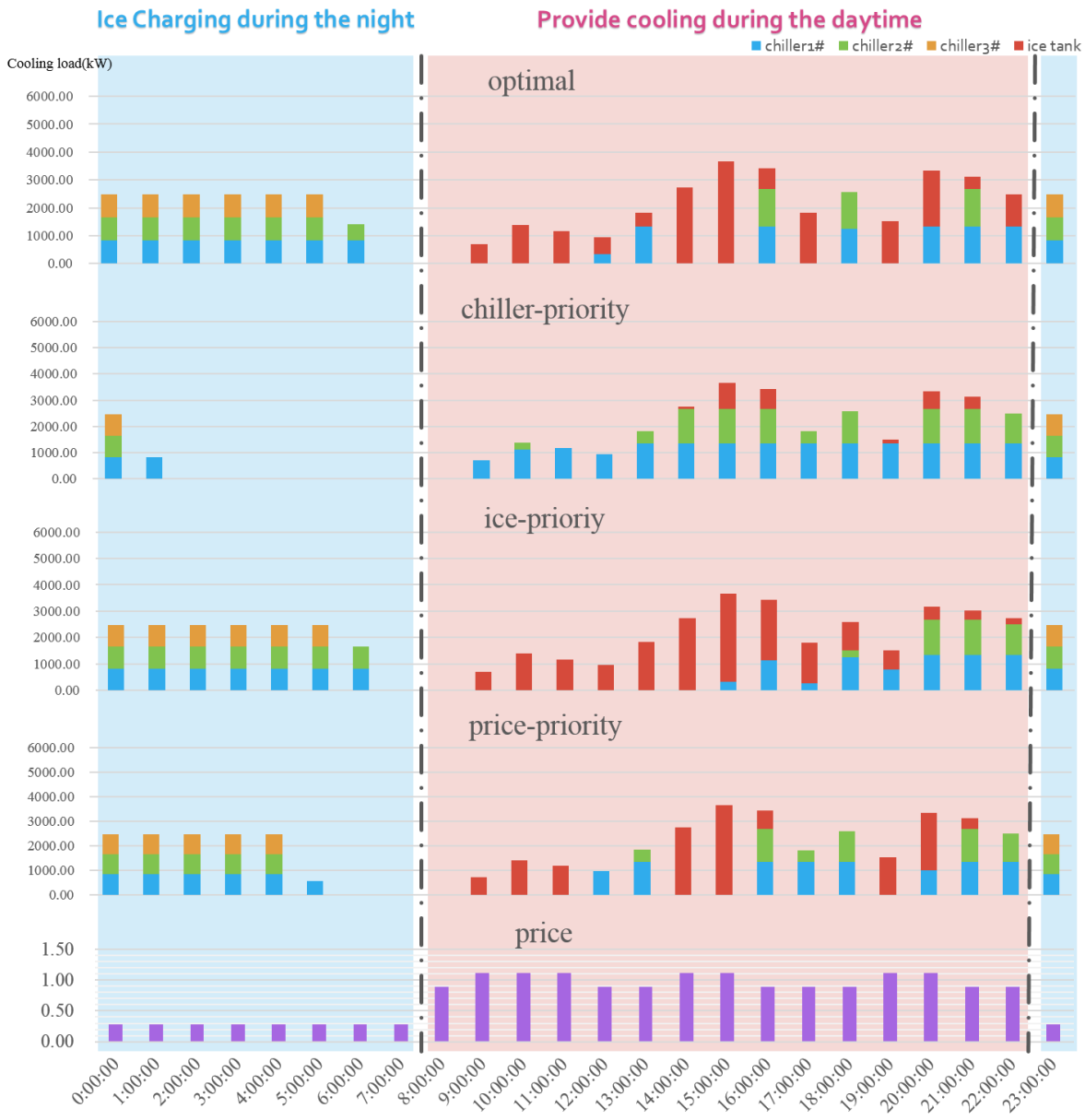

Figure 10 Calculated allocation of cooling loads by different control strategies under the minimum-load scenario

Figure 11 shows the electricity consumption for different control strategies under the minimum-level load scenario. Electricity consumption distributions for the current and price-priority strategies were similar, which suggests that the current control strategy is strongly tied to variation in the electricity rate. Most electricity consumption in the optimal strategy is attributable to the chillers, occurring when the electric rate was at a lower level. Thus, the optimal strategy realized the objective to minimize the total energy costs by taking full advantage of the electricity price distribution.

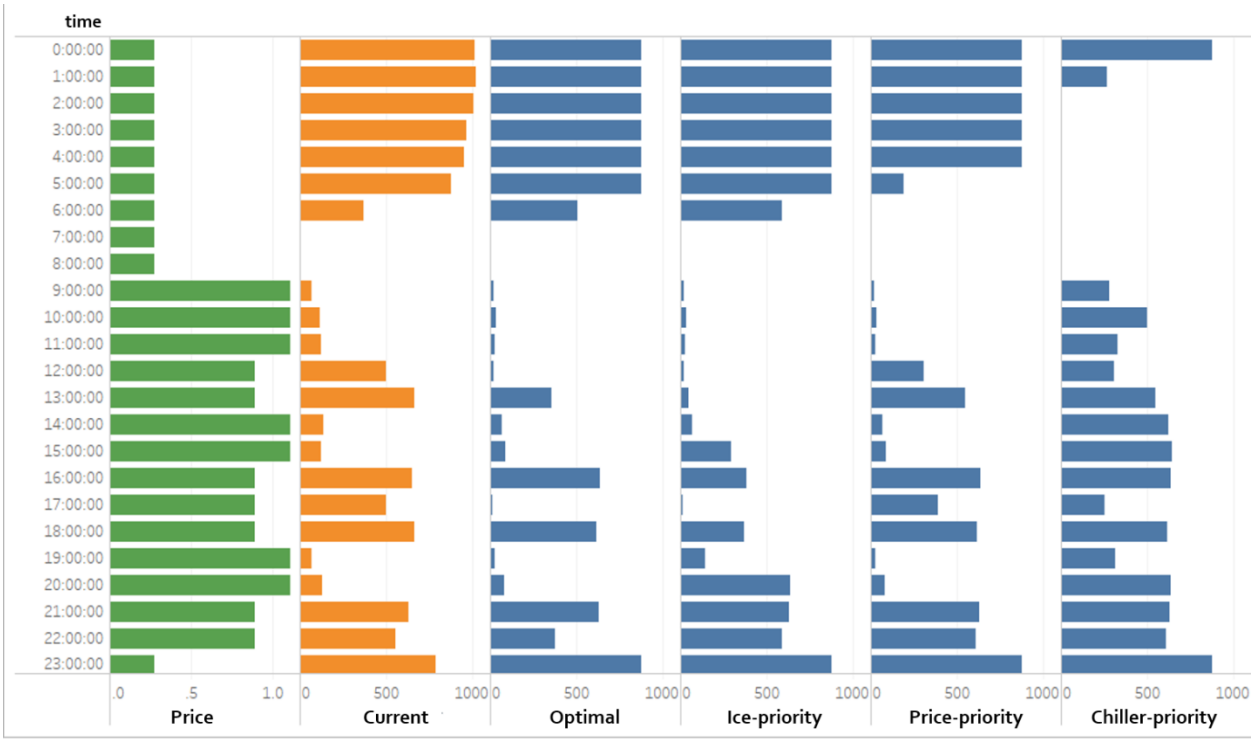

Figure 11 Electricity consumption of different control strategies under the minimum-load scenario

4.1.2. Average level of cooling loads

Figure 12 shows the calculated allocation of cooling load for different control strategies under the average-level load scenario; associated daily operating costs can be seen in column B of Table 3. Here, the optimal strategy saves up to 6.0% of energy costs compared to the current strategy; moreover, the cooling load satisfied by the chillers and ice tank was well allocated in the optimal strategy according to the electricity price profile. Additionally, chillers in the optimal strategy typically operated under full load conditions, maximizjng their efficiency. Operating costs were highest for the chiller-priority strategy, and the ice-storage was only 33% utilized.

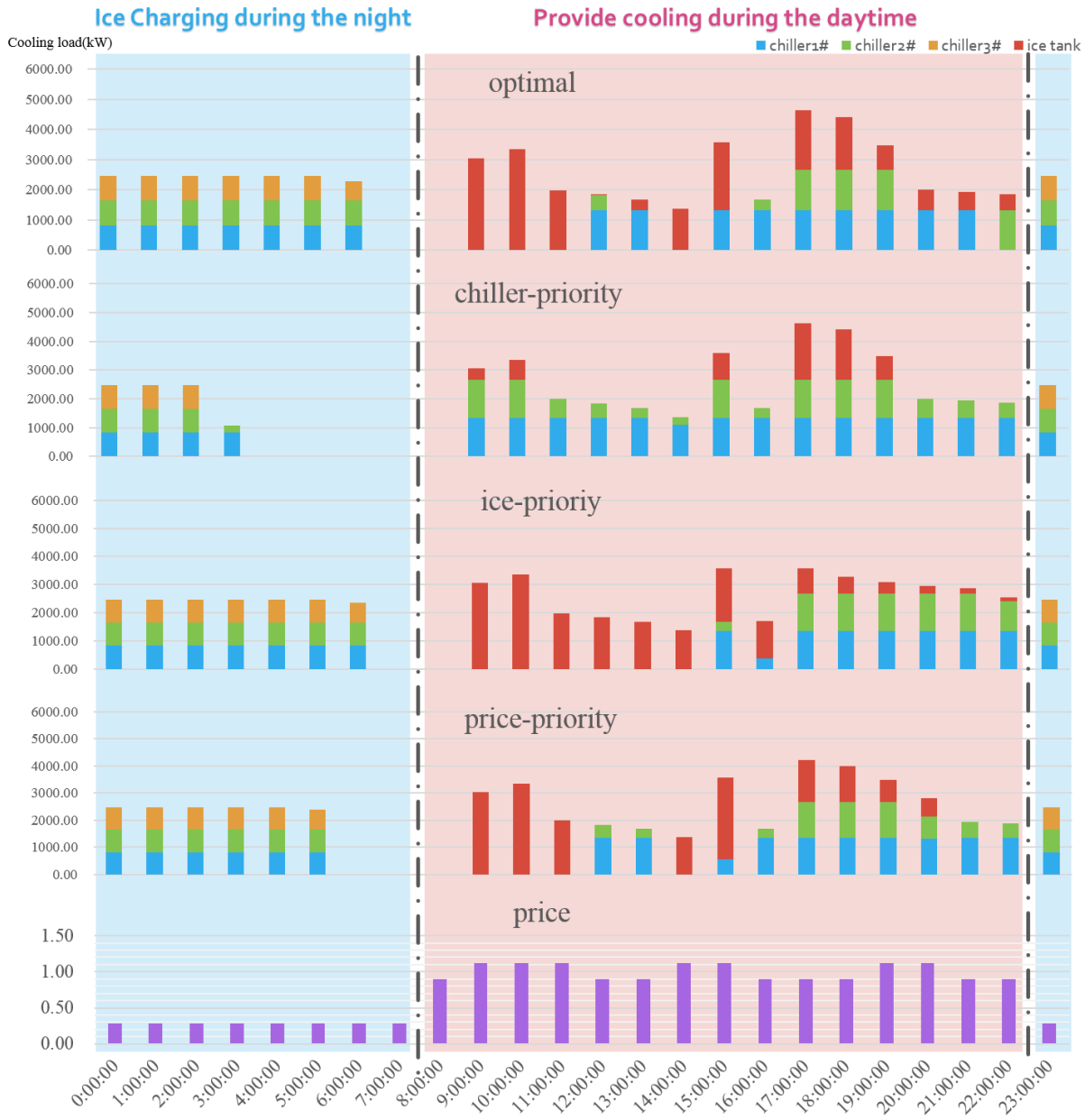

Figure 12 Calculated allocation of cooling loads by different control strategies under the average-load scenario

For the ice-priority and price-priority strategies, the cooling demand during the afternoon was not completely met, as chiller operation was normally limited to two at a time. Indeed, the total capacities of the two chillers were insufficient to satisfy cooling demand after the ice had been used; this constitutes a significant limitation of both the ice-priority and price-priority strategies. It is noted that the unmet cooling load for a given hour was counted in the next hour, and under rare circumstances when the cooling load was not met by the end of a day, the unmet cooling load was ignored and not counted on the next day. Although the operating costs for these two strategies were similar to that of the optimal one, results for these strategies

demonstrate that occupant thermal comfort could decline when up to 20% of cooling demand was not met in a given hour. However, if a third chiller is activated during these hours, the remaining cooling demand can be fully met; the total costs for the strategies under this assumption are shown in column B of Table 4. Here, it is seen that the optimal strategy still saves energy costs when compared to the other three heuristic strategies, specifically: 3.75% lower energy costs than the ice-priority strategy, 4.34% lower energy costs than the price-priority strategy, and 20.29% lower energy costs than the chiller-priority strategy. The advantage of the optimal strategy is obvious when considering both the energy cost saving potential and the satisfaction of the occupants' thermal comfort.

Table 4 Total energy costs (RMB) of different control strategies under three scenarios (all three chillers can operate if needed to meet the cooling loads)

	Minimum load (A)	**Average load (B)**	**Maximum load (C)**
Date	October 10	July 2	August 5
Current	5951.00	7563.66	8228.46
Optimal	5309.47	7113.01	7757.34
Chiller priority	7923.82	8922.32	9268.26
Ice priority	5758.55	**7389.78***	**7899.89***
Price priority	5831.59	**7435.57***	**8108.43***

* These numbers are the updated energy costs for the ice-priority and price-priority strategies under the B and C scenarios, compared with Table 3.

Figure 13 shows the electricity consumption for different control strategies under the average-level load scenario. Here, the third chiller was allowed to operate when the first two chillers did not meet the cooling demand. The distribution of the electricity consumption for the current and price-priority strategies is similar. For the optimal strategy, the chillers consumed the most electricity when the electricity rate was lower, which resulted in the lowest energy costs among the strategies.

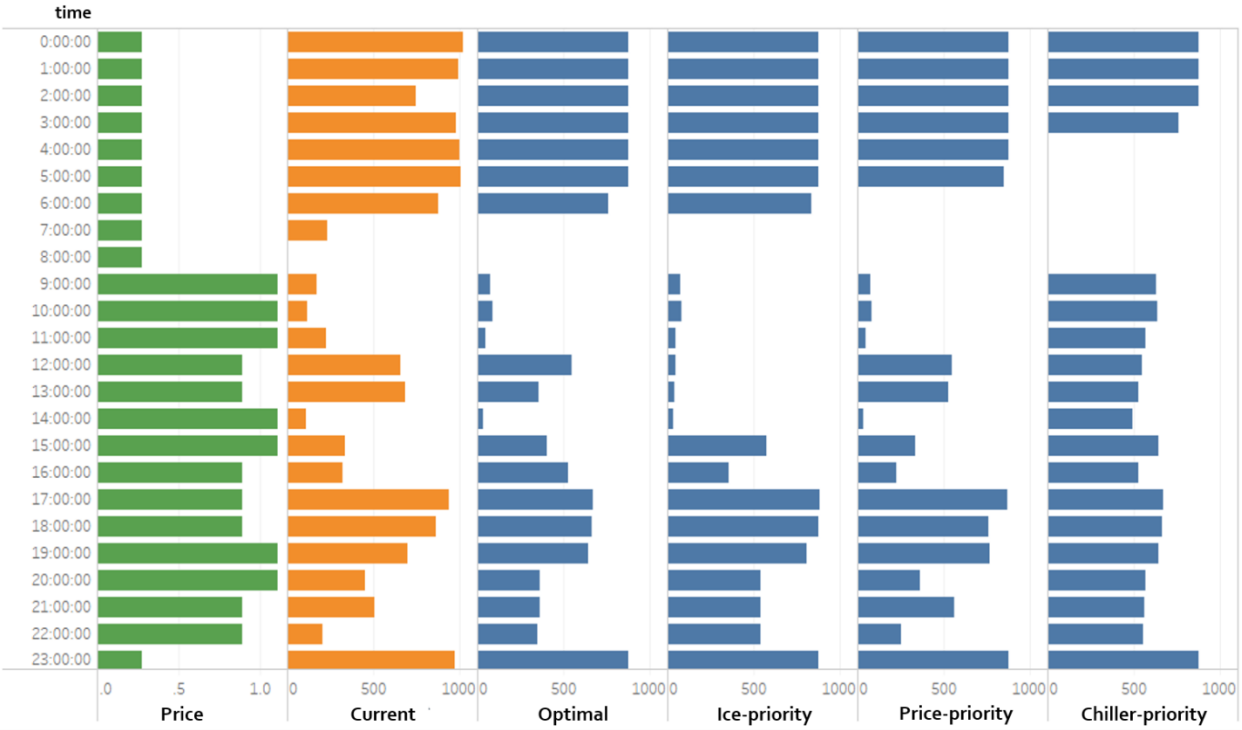

Figure 13 Electricity consumption by different control strategies under the average-load scenario

4.1.3. Maximum level of cooling loads

Figure 14 shows the calculated allocation of cooling loads by different control strategies under the maximum-level load scenario. The daily operating energy cost can be seen in column C of Table 3. Compared to the current strategy, the optimal strategy can save up to 5.7% of energy costs by effectively allocating cooling loads and running the chillers at a higher efficiency (e.g., under higher load ratio conditions). Indeed, under the optimal strategy, the chillers operate at nearly full load during operating hours, which corresponds to a much higher efficiency in the performance curves for the chiller. For the chiller-priority strategy, the ice-storage system was utilized up to about 50%, and the operating costs remained the highest compared to the other strategies. As aforementioned, the limitations of the ice-priority and price-priority strategies become more apparent when the daily cooling load is elevated. Here, occupant thermal comfort declines when up to 40% and 30% of hourly cooling demand is not met under the ice-priority and price-priority strategies, respectively. In fact, under the ice-priority strategy, the total cooling load was not met until the end of the day. After activating the third chiller to help meet the remaining cooling load under these strategies, operating costs increased greatly, as shown in column C of Table 4. Here, the optimal strategy still saves energy costs relative to the other strategies specifically: 1.80% lower energy costs than the ice-priority, 4.33% lower energy costs than the price-priority, and 16.30% lower energy costs than the chiller-priority.

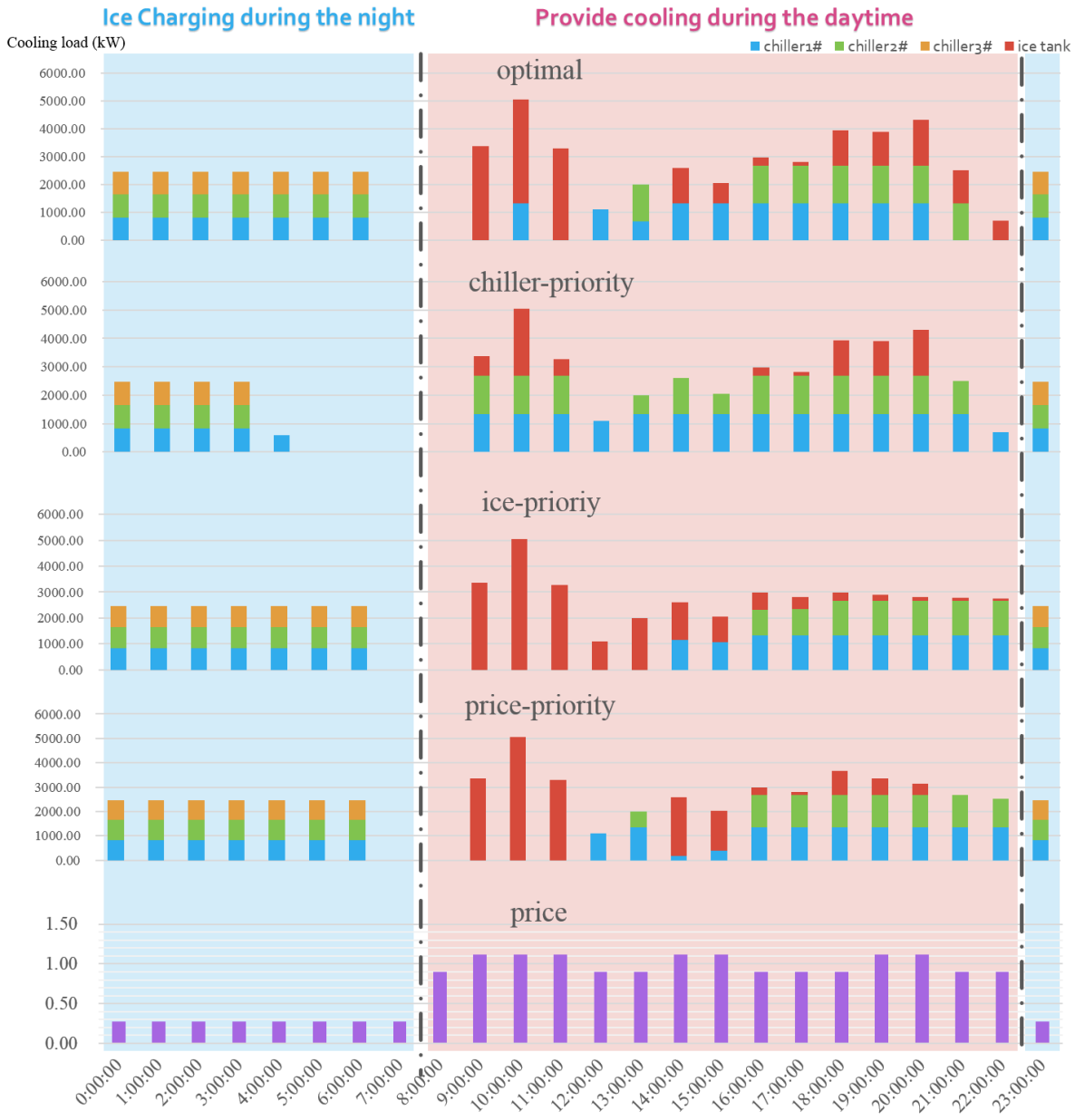

Figure 14 Calculated allocation of cooling loads by different control strategies under the maximum-load scenario

Figure 15 shows the electricity consumption for different control strategies under the maximum-level load scenario. Here, the third chiller was allowed to operate when the cooling demand was not met by the operation of two chillers. The distribution of electricity consumption for the current and price-priority strategies is similar, though the usage rate of the chillers under the current strategy is somewhat higher than that of the price-priority strategy. For the optimal strategy, the chillers consumed the most electricity when the electricity rate was lower, which resulted in the lowest energy costs among the strategies.

Figure 15 Electricity consumption of different control strategies under the maximum-load scenario

4.1.4. Summary of the daily analysis

Comparing the control patterns and total energy costs under various operation strategies, the optimal strategy developed in this paper was shown to be most effective in allocating the operation modes of chillers and ice tank among all five strategies, including the current one. Specifically, total energy costs under the optimal strategy are reduced by 5.7%-11.3% compared to a modified price-priority strategy (in current use), and by 16.3%-33.0% compared to a rule-based chiller-priority strategy. On one hand, the ice storage was not fully discharged under the current strategy; the strategy therefore misses a significant opportunity to reduce energy costs. Conversely, when the proposed optimal strategy was used, ice storage was typically fully charged during the night and fully discharged during the daytime; this not only helped reduce the usage of the chillers, but also enhanced the operating efficiency of the chiller group. In the heuristic storage-priority strategy, ice storage was fully used; however, the total cooling demand was not met for majority of the days under this strategy, likely sacrificing occupant comfort in the shopping mall. Conversely, the optimal strategy achieves energy cost savings while still meeting the total daily cooling demand. Moreover, as mentioned, the optimal strategy better allocates the operating modes of chillers and ice tank, which helps to avoid operating the chillers during high electricity price periods.

Finally, by calculating results under three cooling demand scenarios, the savings potential of the optimal strategy was shown to vary based on the level of the daily total cooling demand.

Specifically, the lower the daily cooling demand, the higher the daily cost savings for the optimal strategy were when compared to the current modified strategy.

4.2. Monthly analysis

Monthly results were also calculated and analyzed for the five control strategies. Figure 16 shows the total energy costs in July, August, and September, assuming that only up to two chillers could operate at the same time. The total cooling demand in August and September were the highest and lowest within these three months, respectively. Compared to the current strategy, the optimal strategy can save 7.7%, 6.3%, and 9.3% of the current energy costs in July, August, and September, respectively. The chiller-priority strategy always cost the most as it does not take full advantage of the ice-storage system. As for the ice-priority strategy, in July, there were five days when the total cooling demand was not met by the end of the day. The unsatisfied cooling demand accounted for 11.7% of the total cooling demand. In August, there were eight days in total when the daily cooling demand was not met. The unsatisfied cooling demand accounted for 16.2% of the total cooling demand. In September, the cooling demand for each day was met; however, in certain typical hours, the unsatisfied cooling load still rose to 2.7% of the hourly cooling demand. Similar problems applied to the price-priority strategy; in July and August, the unmet cooling loads accounted for 3.1% and 5.5% of the total cooling loads, respectively. Moreover, under the price-priority strategy, there were two days when the total daily cooling demand was not met by the end of the day in August.

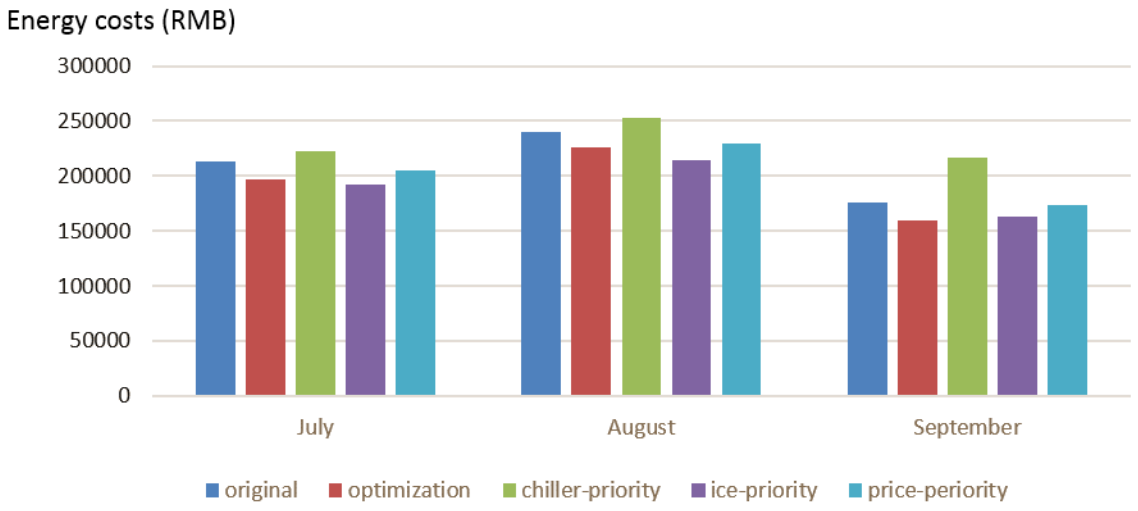

Figure 16 Monthly energy costs of different control strategies in July, August and September (maximally two chillers operating)

As aforementioned, if the third chiller was activated during those hours when the cooling load was not met, the remaining cooling demand could be fully met. The monthly total costs of

different strategies were also calculated under this scenario, and results are shown in Figure 17. Clearly, the optimal strategy still saves energy costs compared to the current control strategy and the other three heuristic strategies, even when allowing the other strategies to fully meet the cooling demand and satisfy occupant thermal comfort.

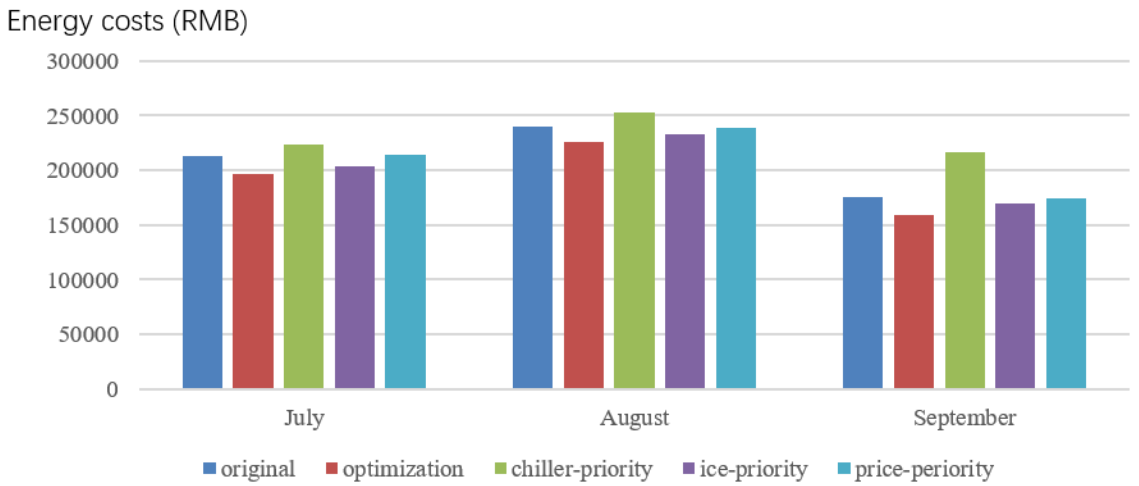

Figure 17 Monthly energy costs of different control strategies in July, August and September (all three chillers can operate if needed to meet the cooling loads)

4.3. Validation of the hourly cooling load prediction model

The cooling load dataset we have contains 1,708 samples of time-stamped web-bulb temperature and cooling load data collected in Shenzhen, lasting about 71 days. We used 750 samples for training and the rest for the validation of the model. We compared our GPR model's predictive performance for the testing dataset against that of other regression methods studied in the previous literature, including linear regression (LR), Generalized Regression Neural Network (GRNN) [31], Support Vector Machine Regression (SVMR) [32], and Random Forest Regression (RFR) [33]. We use MATLAB built-in functions, fitlm, newgrnn, fitrsvm, and TreeBagger to implement LR, GRNN, SVMR, and RFR, respectively. Our GPR model is implemented using the GPML toolbox [34]. Predictive performance was evaluated via three commonly used measures, namely: Relative Absolute Error (RAE), Relative Root Mean Square Error (RRMSE), and R-squared value (R^2), which are defined as follows:

$$RAE = 100 \times \frac{\frac{1}{N_t}\sum_{i=1}^{N_t}|e_i|}{\frac{1}{N_t}\sum_{i=1}^{N_t} y_i^{test}} \quad \text{Eq. 22}$$

$$RRMSE = 100 \times \frac{\sqrt{\frac{1}{N_t}\sum_{i=1}^{N_t} e_i^2}}{\frac{1}{N_t}\sum_{i=1}^{N_t} y_i^{test}} \quad \text{Eq. 23}$$

$$R2 = 100 \times \left(1 - \frac{\frac{1}{N_t}\sum_{i=1}^{N_t} e_i^2}{\frac{1}{N_t}\sum_{i=1}^{N_t}\left(y_i^{test} - \frac{1}{N_t}\sum_{i=1}^{N_t} y_i^{test}\right)^2} \right) \qquad \text{Eq. 24}$$

where $e_i = y_i^{test} - y_i^{true}$ is the difference between the prediction of ith test sample y_i^{test} and its true value y_i^{true}. RAE and RRMSE measure the deviation of a prediction from the true value, where RAE focuses more on the performance of predicting the general trend, while RRMSE is more sensitive to the prediction error of extreme target values. Finally, R^2 measures the percentage of the target variation that is explained by the model; accordingly, a higher R^2 value is more desirable.

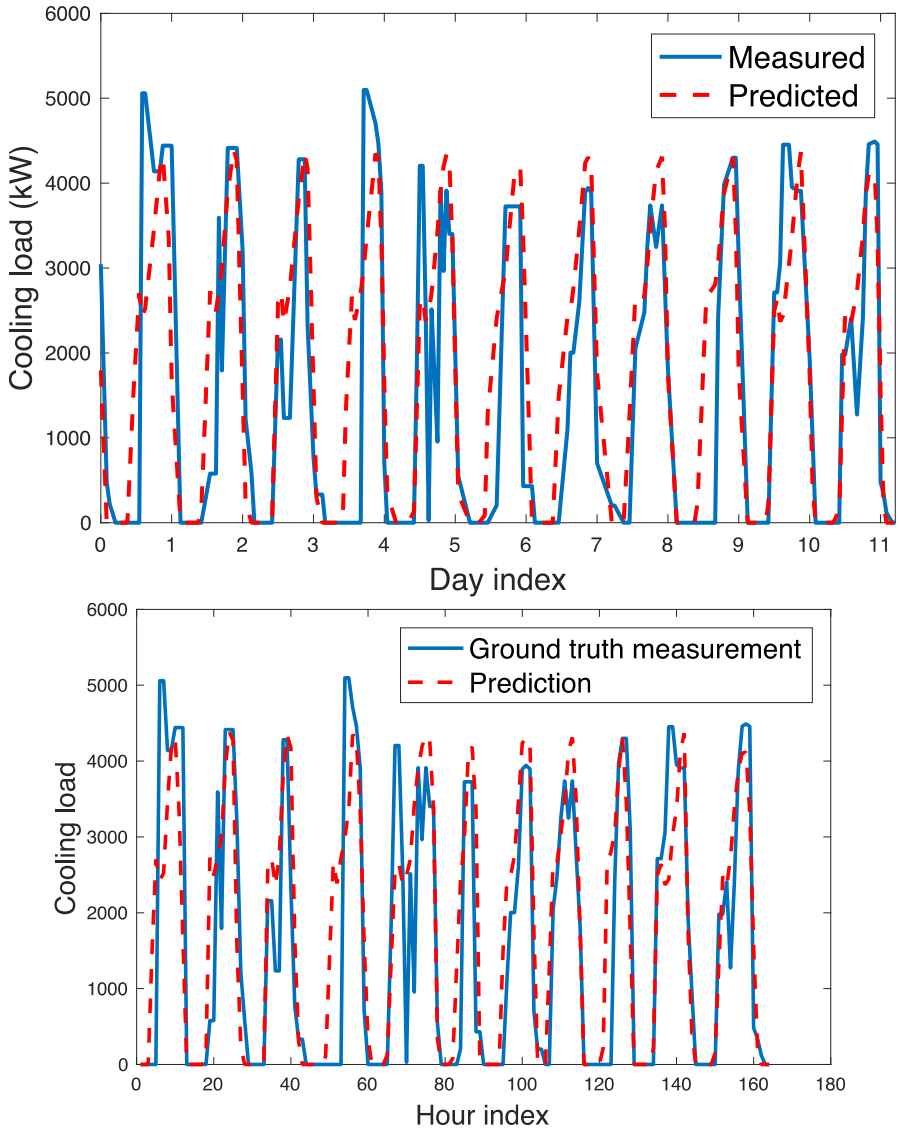

Figure 18 Visualization of cooling load prediction during a randomly chosen time window

Figure 18 visualizes the load prediction results and the corresponding ground truth measurements during a randomly chosen time window. From this, it is evident that the GPD

prediction effectively captures the trend in ground truth measurements. Table 5 summarizes the load prediction performance of our GPR method as well as other methods; the table demonstrates that GPR significantly outperforms the other prediction method, under all metrics. Note that simple linear regression and SVM regression methods are relatively ineffective in predicting the cooling load variation.

Table 5 Comparison of the prediction performance of different load prediction algorithms

Prediction Algorithm	RAE (%)	RRMSE (%)	R2 (%)
LR	62.86	89.01	24.77
GRNN	53.75	82.27	35.73
SVMR	67.53	98.68	7.53
RFR	48.81	69.51	54.12
GPR	**5.37**	**64.79**	**60.13**

5. Discussion

By comparing the operational energy cost of five control strategies, it was demonstrated that the rate of the ice tank plays a key role in reducing the energy costs of a TES system. In the optimal strategy, considered the most economical and effective way to control the TES system, the ice tank was always fully charged during the night and fully discharged during the daytime. It can be inferred that a larger storage capacity would favor more operating cost savings for the developed optimal strategy, especially for those days when the total cooling demand exceeds the designed storage capacity. Theoretically speaking, when it comes to the operation of an existing TES system, there are two keys to achieving operating cost savings: (1) better allocate the cooling demand between the chillers and the ice tank according to the time-of-use electricity rate, and (2) control the chillers such that they operate under full load conditions (or as high as possible) to increase their efficiency.

When analyzing real operation data from a shopping mall in this work, statistics suggest that the total daily cooling demand on the majority of the days exceeded the cooling capacity of the designed ice tank. Thus, chillers were required to operate to help meet the cooling demand even during high electricity rate periods. Accordingly, during the design of a TES system, statistical analysis is needed to better predict the daily cooling demand, considering weather patterns, building type, occupant thermal comfort, and building operation. The capacities of the ice tank and the chiller group should then be carefully determined based on the average and maximum cooling demand, in order to realize a larger energy cost saving potential. In addition,

the capacities of the ice tank and chillers determine their initial capital cost, which should be considered in an optimal design.

As aforementioned, previous optimization studies on TES systems have mostly focused on physically modeling building thermal performance. In this work, data-driven analysis and modeling were used to first clearly understand the system's current operating performance and control strategy, which improves the accuracy of cooling load predictions as well as the reliability of the optimization results. Similar to the previous results, the optimal strategy takes advantage of better allocating the usage of chillers and storage function according to a varying electricity price and peak power contraction. Thus, to achieve a practical optimal strategy, the optimization problem should be carefully formulated considering all related constraint conditions.

It should be noted that there are limitations in this study, namely: (1) the performance parameters of the cooling and ice-storage system were analyzed from the datasets measured in a real shopping mall in Shenzhen city in China; thus, the optimal strategy determined in this work is most applicable to this type of TES system. However, the data analytics and optimization methodology is generic and applicable to other types of TES systems in other types of commercial buildings; (2) since the chilled water flow rate from the chiller group and the ice tank were not measured separately, the hourly control mode of the current TES system could only be determined by the open status of the valves. This meant that the hourly usage statistics of the chillers and the ice tank could be collected and analyzed, but the exact quantity of the cooling demand for each piece of equipment in the central cooling plant could not be determined. Nevertheless, this paper's comparison of energy consumption to the valves' open status was sufficient to reveal the savings potential of the proposed optimal control strategy.

6. Conclusions

This study used data-driven analytics to understand the operation of an ice–based TES system in a shopping mall and to calculate the system's performance using data measured from meters and sensors that were installed on the system. A novel optimal control strategy was then developed to minimize the system's operating costs; this optimal strategy was compared with three heuristic control strategies. The savings potential of the optimal strategy relative to the heuristic strategies was assessed under three scenarios of cooling demand level using three representative days of data.

Results demonstrated that the current strategy used to operate the TES system was largely based on the distribution of electricity price, and the use of chillers was prioritized over the use of the ice tank. In particular, the ice tank was not fully discharged during the daytime in the current strategy, leaving savings on the table that were captured by the optimal strategy. By analyzing the measured datasets, the performance characteristics of the current TES system were determined; performance and energy cost outcomes for the three heuristic strategies

were also studied. By comparing total energy costs and control patterns across strategies, the optimal strategy was shown to be the most effective in yielding energy cost savings and fully meeting cooling demands needed to satisfy occupant thermal comfort. Specifically, the optimal strategy saved up to 11.3% per day and 9.3% per month in energy costs over the system's current operation strategy. The energy cost savings potential of the optimal strategy was found to depend on the level of total daily cooling demand: when the cooling demand is low, the ice tank is more effectively utilized by fully charging the ice storage during the night and better allocating the cooling demand between the chillers and the ice tank.

A machine learning-based, hourly cooling demand prediction tool will support the deployment of this paper's analytics and optimization techniques in real TES systems. Looking ahead, the optimal strategy presented here will be implemented and tested in the actual TES system of the shopping mall.

Acknowledgments

The authors would like to acknowledge the China Scholarship Council (CSC) for the graduate fellowship. This work is also supported by the Assistant Secretary for Energy Efficiency and Renewable Energy of the United States Department of Energy under Contract No. DE-AC02-05CH11231.

References

[1] Sadineni SB, Boehm RF. Measurements and simulations for peak electrical load reduction in cooling dominated climate. Energy 2012; 37(1): 689–97.

[2] Sun Y, Wang S, Xiao F, Gao D. Peak load shifting control using different cold thermal energy storage facilities in commercial buildings: a review. Energy Convers Manage 2013; 71: 101–14.

[3] Oro E, de Gracia A, Castell A, Farid M, Cabeza LF. Review on phase change materials (PCMs) for cold thermal energy storage applications. Appl Energy 2012; 99: 513-33.

[4] Potter RA, Weitzel DP, King DJ. Study of operational experience with thermal storage systems. ASHRAE Trans 1995; 101: 549–57.

[5] Palacio SN, Valentine KF, Wong M, Zhang KM. Reducing power system costs with thermal energy storage. Appl Energy 2014; 129: 228-37.

[6] M.S. Soler, C.C. Sabate, V.B. Santiago, F. Jabbari, Optimizing performance of a bank of chillers with thermal energy storage, Applied Energy. 172 (2016) 275-285.

[7] de Falco M, Capocelli M, Giannattasio A. Performance analysis of an innovative PCM-based device for cold storage in the civil air conditioning. Energ Buildings 2016; 12: 1-10.

[8] Gupta A, Anand Y, Tyagi SK, Anand S. Economic and thermodynamics study of different cooling option: A review. Renew Sust Energ Rev 2016; 62: 164-94.

[9] Sanaye S, Shirazi A. Thermo-economic optimization of an ice thermal energy storage system for air-conditioning applications. Energ Buildings 2013; 60: 100-09.

[10] Henze GP, Krarti M, Brandemuehl MJ. Guidelines for improved performance of ice storage systems. Energ Buildings 2013; 35: 111-27.
[11] MacPhee D, Dincer I. Performance assessment of some ice TES system. Int J Therm Sci 2009; 48: 2288-99.
[12] Cui B, Gao D, Xiao F, Wang SW. Model-based optimal design of active cool thermal energy storage for maximal life-cycle cost saving from demand management in commercial buildings. Appl Energy 2017; 201: 382-96.
[13] Candanedo JA, Dehkordi VR, Stylianou M. Model-based predictive control of an ice storage device in a building cooling system. Appl Energy 2013; 111: 1032-45.
[14] Ma Y, Borrelli Y, Hencey B, Packard A, Bortoff S. Model predictive control of thermal energy storage in building cooling systems, in: Proceedings of the 48th IEEE Conference on Decision and Control, 2009, pp. 392–397.
[15] Lee WS, Chen Y, Wu TH. Optimization for ice-storage air-conditioning system using particle swarm algorithm. Appl Energy 2009; 86(9): 1589–95.
[16] Zhou Z, Liu P, Li Z, Ni W. An engineering approach to the optimal design of distributed energy systems in China. Appl Therm Eng 2013; 53: 387–96.
[17] Lu YH, Wang SW, Sun YJ, Yan CC. Optimal scheduling of buildings with energy generation and thermal energy storage under dynamic electricity pricing using mixed-integer nonlinear programming. Appl Energy 2015; 147: 49-58.
[18] Vetterli J, Benz M. Cost-optimal design of an ice-storage cooling system using mixed-integer linear programming techniques under various electricity tariff schemes. Energ Buildings 2012; 49: 226–34.
[19] Ruan YJ, Liu QR, Li ZW, Wu JZ. Optimization and analysis of building combined cooling, heating and power (BCHP) plants with chilled ice thermal storage system. Appl Energy 2016; 179: 738-54.
[20] Sanaye S, Fardad A, Mostakhdemi M. Thermo economic optimization of an ice thermal storage system for gas turbine inlet cooling. Energy 2011; 36: 1057–67.
[21] Wang J, Zhai Z, Jing Y, Zhang C. Particle swarm optimization for redundant building cooling heating and power system. Appl Energy 2010; 87: 3668–79.
[22] Ashouri A, Fux SS, Benz MJ, Guzzella L. Optimal design and operation of building services using mixed-integer linear programming techniques. Energy 2013; 59: 365–76.
[23] S. Fazlollahia, G. Beckera, F. Maréchal, Multi-objectives, multi-period optimization of district energy systems: II—Daily thermal storage, Computers and Chemical Engineering. 71 (2014) 648–662.
[24] Yun H, Li W. Optimization and analysis of distributed energy system with energy storage device. Energy Procedia 2011; 12: 958–65.
[25] Ooka R, Ikeda S. A review on optimization techniques for active thermal energy storage control, Energ Buildings 2015; 106: 225-33.
[26] Shaikh PH, Nor NBM, Nallagownden P, Elamvazuthi I, Ibrahim T. A review on optimized control systems for building energy and comfort management of smart sustainable buildings. Renew Sust Energ Rev 2014; 34: 409-29.
[27] Wang SW, Ma ZJ. Supervisory and optimal control of building HVAC system: A review. HVAC&R Res 2008; 14(1): 3-32.

[28] Blum M, Riedmiller M. Electricity demand forecasting using Gaussian processes. Power 2013; 10: 104.
[29] Rasmussen CE. Gaussian processes for machine learning. 2006.
[30] Nguyen-Tuong D, Seeger M, Peters J. Model learning with local gaussian process regression. Adv Robot 2009; 23(15): 2015-34.
[31] Ben-Nakhi AE, Mahmoud MA. Cooling load prediction for buildings using general regression neural networks. Energy Convers Manage 2004; 45(13): 2127-41.
[32] Li Q, Meng Q, Cai J, Yoshino H, Mochida A. Applying support vector machine to predict hourly cooling load in the building. Appl Energy 2009; 86(10): 2249-56.
[33] Dalipi F, Yayilgan SY, Gebremedhin A. Data-driven machine-learning model in district heating system for heat load prediction: A comparison study. Appl Computational Intelligence Soft Computing 2016.
[34] GPML toolbox. http://www.gaussianprocess.org/gpml/code/matlab/doc/.